IRSTI 29.15.17 https://doi.org/10.26577/RCPh.2021.v79.i4.03

B.M. Sadykov[1*], M. Nassurlla[1], B.A. Duisebayev[1], T.K. Zholdybayev[1], S.B. Sakuta[2], Y. Bugybayev[3]

[1]Institute of Nuclear Physics, Kazakhstan, Almaty,
[2]National Research Center "Kurchatov Institute", Russia, Moscow
[3]L.N. Gumilyov Eurasian National University, Kazakhstan, Nur-Sultan
*e-mail: sadykovbm@inp.kz

SCATTERING PROCESSES OF HELIUM NUCLIDES ON NUCLEI ^{28}SI

Experimental data on elastic and inelastic scattering of 50.5 MeV α-particles and 60 MeV ^{3}He ions by ^{28}Si nuclei were analyzed within the framework of the standard optical model of the nucleus, in which the effect of inelastic channels is taken into account by the phenomenological introduction of an imaginary absorbing part into the interaction potential between colliding nuclei. The optimal values of the internuclear interaction potential obtained as a result of the theoretical analysis were used to study the cross sections for inelastic scattering of helium ions with the excitation of the 1.78 and 4.61 MeV states of the nucleus under study. From the analysis by the channel coupling method, where the calculation was performed taking into account both elastic and inelastic channels, the value of the quadrupole deformation parameter for α-particles $\beta_2 = 0.37$ and for ^{3}He ions $\beta_2 = 0.49$ was determined. Optimal agreement between the calculated values and experimental data was achieved by varying the parameters V, W, and β_2. The found parameters agree with the previously obtained values from the scattering of protons, deuterons and α-particles. Taking into account only the quadrupole deformation extracted from the $0^+ - 2^+$ bond, a good description of all three experimental data on elastic and inelastic scattering of the cross sections was achieved.

Key words: elastic and inelastic scattering, optical model, optical potential, coupled channel method.

Б.М. Садыков[1*], М. Насурлла[1], Б.А. Дуйсебаев[1], Т.К. Жолдыбаев[1], С.Б. Сакута[2], Е. Бугыбаев[3]

[1]Ядролық физика институты, Қазақстан, Алматы қ.
[2]«Курчатов институты» ұлттық ғылыми орталығы, Ресей, Мәскеу қ.
[3]Л.Н. Гумилев атындағы Еуразия ұлттық университеті, Қазақстан, Нұр-Сұлтан қ.
*e-mail: sadykovbm@inp.kz

^{28}Si ядроларынан гелий нуклидтерінің шашырау процестері

50.5 МэВ α-бөлшектері мен 60 МэВ ^{3}Не иондарының ^{28}Si ядроларынан серпімді және серпімсіз шашырауы туралы эксперименттік мәліметтер ядроның стандартты оптикалық моделі шеңберінде талданды, онда серпімсіз арналардың әсері соқтығысатын ядролардың өзара әрекеттесу потенциалына феноменологиялық жорамал сіңіргіш бөлігін енгізу арқылы есептелді. Теориялық талдау нәтижесінде алынған ядролық өзара әрекеттесу потенциалының оңтайлы мәндері зерттелетін ядроның 1.78 және 4.61 МэВ қозған күйлерінен гелий иондарының серпімсіз шашырауына арналған қималарды зерттеу үшін пайдаланылды. Каналды байланыстыру әдісімен талдаудан, серпімді және серпімсіз арналарды ескере отырып есептеулер жүргізілді, α-бөлшектері үшін квадруполды деформация параметрінің мәні $\beta_2 = 0.37$ және ^{3}Не иондары үшін $\beta_2 = 0.49$ анықталды. Есептелген мәндер мен эксперименттік деректер арасындағы оңтайлы келісімге V, W және β_2 параметрлерін өзгерту арқылы қол жеткізілді. Табылған параметрлер протондардың, дейтерондардың және α-бөлшектердің шашырауынан бұрын алынған мәндермен сәйкес келеді. $0^+ - 2^+$ байланысынан алынған квадруполды деформацияны ғана ескере отырып, көлденең қималардың серпімді және серпімді емес шашырауы туралы барлық үш тәжірибелік мәліметтердің жақсы сипаттамасына қол жеткізілді.

Түйін сөздер: серпімді және серпімсіз шашырау, оптикалық модель, оптикалық потенциал, байланысқан канал әдісі.

Б.М. Садыков[1*], М. Насурлла[1], Б.А. Дуйсебаев[1],
Т.К. Жолдыбаев[1], С.Б. Сакута[2], Е. Бугыбаев[3]

[1]Институт ядерной физики, Казахстан, г. Алматы
[2]Национальный исследовательский центр «Курчатовский институт», Россия, г. Москва
[3]Евразийский национальный университет имени Л.Н. Гумилева, Казахстан, г. Нур-Султан
*e-mail: sadykovbm@inp.kz

Процессы рассеяния нуклидов гелия на ядрах ^{28}Si

Экспериментальные данные по упругому и неупругому рассеянию α-частиц с энергией 50,5 МэВ и ионов ^{3}He 60 МэВ на ядрах ^{28}Si анализировались в рамках стандартной оптической модели ядра, в которой влияние неупругих каналов учитывается феноменологическим введением мнимой поглощающей части в потенциал взаимодействия между сталкивающими ядрами. Полученные в результате теоретического анализа оптимальные значения потенциала межъядерного взаимодействия были использованы при исследовании сечений неупругого рассеяния ионов гелия с возбуждением состояний 1,78 и 4,61 МэВ исследуемого ядра. Из анализа методом связи каналов, где расчет выполнялся с учетом как упругого, так и неупругих каналов, определено значение параметра квадрупольной деформации для α-частиц $\beta_2 = 0.37$ и для ионов ^{3}He $\beta_2 = 0.49$. Оптимальное соответствие расчетных величин с экспериментальными данными достигалось варьированием параметров V, W и β_2. Найденные параметры согласуются с ранее полученным значениями из рассеяния протонов, дейтронов и α-частиц. С учетом лишь квадрупольной деформации, извлеченной из $0^+ - 2^+$ связи, достигнуто хорошее описание всех трех экспериментальных данных упругого и неупругого рассеяния сечений.

Ключевые слова: упругое и неупругое рассеяние, оптическая модель, оптический потенциал, метод связанных каналов.

Introduction

The study of experimental data on elastic and inelastic scattering, which contains information on the fundamental properties of colliding nuclei and the mechanisms of their interaction, remains one of the topical areas of nuclear physics.

Particular attention is drawn to the nuclei in the middle of the *sd*-shell because, according to [1, 2], there is a transition from elongated deformation, which is characteristic of nuclei of the first half of the *sd*-shell, to oblate deformation. It is in the region of the silicon core that the quadrupole deformation parameter β_2 changes sign. In most cases the numerical value of the quadrupole deformation was obtained from the analysis of the cross sections for inelastic scattering by the method of distorted waves. However, this method does not take into account the channel coupling effects, which play an essential role for strongly deformed nuclei. The analysis of experimental data on inelastic scattering was carried out by the coupled channel method in this work.

Analysis of data on scattering of α-particles is one of the effective means of studying nuclear deformation, which is due to the relatively simple reaction mechanism. Therefore, a large number of works have been devoted to the scattering of α-particles. In particular, for the ^{28}Si nucleus, the scattering cross sections were measured in a fairly wide range of angles and energies (E_α = 12 – 240 MeV) [3-10].The problem that manifests itself during the plotting of the angular distributions of the cross sections at energies less than 50 MeV was to explain the effect of anomalous scattering at large angles. Attempts have been made to achieve a better description of the experimental data by selecting the optimal parameters of the optical potential and taking into account the contribution of the compound nucleus. However, these actions did not lead to a theoretically substantiated description of scattering in a wide range of targets and energies. At the same time, calculations of the differential cross sections for scattering of alpha particles by *1p*-shell nuclei, carried out taking into account the link between the channels and the contribution of the cluster transfer mechanism, made it possible to describe the behavior of the angular distributions in the full angular range [11, 12].

A similar situation is observed in the analysis of data on the scattering of ^{3}He ions during their interaction with ^{28}Si nuclei. Elastic scattering of ^{3}He was studied at energies of 35.3 MeV [13], 35.7 MeV [14], 46 MeV [15], 217 MeV [16], and 450 MeV [17] and was analyzed within the framework of an optical model in which the deformation of nuclei was not taken into account. Only in [15] did the measurements include inelastic scattering, which made it possible to derive the values of the quadrupole deformation parameters from the analysis of experimental data. Note that the correct reproduction of the angular distributions of scattering of α-particles and ^{3}He ions by *1p*- and *sd*-shell nuclei with deformation parameters consistent with their theoretical values was achieved in [12, 18], where the calculations were performed using the coupled channel method.

Materials and methods

The measurements were performed on the U-150M isochronous cyclotron of the Institute of Nuclear Physics [19] with beams of helium ions accelerated to energies of 50.5 MeV (for α-particles) and 60 MeV (for ^{3}He).

A self-supporting, produced by thermal evaporation, thin film of enriched isotope ^{28}Si – 92.23 % with an average effective thickness of 0.59 mg/cm^2 was used as a target nucleus. The target thickness was determined by the weighing method, as well as by the energy loss of α-particles of the radioactive source ^{241}Am – ^{243}Am – ^{244}Cm with an accuracy of 6 – 9 %.

Registration and identification of scattered particles was carried out by a spectrometric unit consisting of two surface-barrier silicon detectors (ΔE – E – method) from ORTEC: transit – ΔE and total absorption – E, the thicknesses of which were chosen depending on the energy of the scattered particles and varied for the E counter in the range from 500 microns to 1 mm, and for the ΔE counter – from 18 microns to 100 microns. The total energy resolution of the spectrometric channel was ~ 500 keV and was mainly determined by the energy distribution of the primary beam of accelerated helium ions. After preliminary selection in terms of time and amplitude in the spectrometric channels, pulses from the (ΔE – E) telescope entered the input of the multivariate programmed analysis system with identification of the products of nuclear reactions [20].

The angular distributions of scattered ions on the ^{28}Si isotope were measured in the angular range 12 – 172^0 in the laboratory coordinate system with a step of ~ 2 – 3^0.The total error of the measured cross sections did not exceed 10%, where the contribution of statistical errors is (1 – 3) % for inelastic scattering and the calibration error of the current integrator (~ 1%).

Results and Discussion

The analysis was carried out within the framework of the optical model. The calculations used phenomenological potentials with volume and surface absorption in the form

$$U(r) = -Vf(x_V) - i\left[Wf(x_W) - 4W_D\frac{d}{dx_D}(x_D)\right] + V_C(r), \quad (1)$$

where V, W, W_D are depths of real and imaginary potentials with volume (W) and surface (D) absorption, which are responsible for the nuclear interaction; V_C is the Coulomb potential of a uniformly charged sphere with radius $R_C = r_C A^{1/3}$; $f(x_i)$ is Woods-Saxon form factor with geometric parameters of radius $R_i = r_i A^{1/3}$ and diffusion a_i ($i=V, W, D$)

$$f(r) = \left[1 + exp\left(\frac{r - r_i A^{1/3}}{a_i}\right)\right]^{-1}. \quad (2)$$

Calculations were performed using the SPI-GENOA program [21]. When searching for the optimal values of the parameters of the potentials, the literature data obtained earlier in the study of elastic scattering at different energies of α-particles [22, 23] and ^{3}He ions [24, 25] were used as starting data.

Figure 1 show comparisons of the calculated elastic scattering cross sections for α-particles and ^{3}He with experimental data.

The parameters of the optical potential were selected in such a way as to achieve the best agreement between theoretical calculations and experimental data. Automatic search for the optimal parameters of the optical potential was carried out by minimizing the value:

$$\chi^2 = \sum_{i=1}^{N}\left[\frac{\sigma^E(\theta_i) - \sigma^T(\theta_i)}{\Delta\sigma^E(\theta_i)}\right]^2, \quad (3)$$

where N is number of points; $\sigma^E(\theta_i)$, $\sigma^T(\theta_i)$ are experimental and theoretical differential cross sections for elastic scattering of particles at an angle θ_i; $\Delta\sigma^E(\theta_i)$ is error $\sigma^E(\theta_i)$.

When choosing the optimal parameters of the optical potential, we were guided not only by the value of χ^2, but also by the value of the volume integral of the real part V_0 of the optical potential, defined as:

$$J_V = -\left(\frac{1}{A_p A_t}\right)\int V(r) 4\pi r^2 dr \quad (4)$$

where A_p and A_t are the mass numbers of the incident particle and target nucleus, the value of which should be close to the corresponding value of the nucleon-nucleon interaction potential, equal to ≈ 400 MeV•fm^3[26]. The Coulomb radius parameter was taken to be $r_c = 1.3$ *fm*. In the course of this analysis on ^{28}Si nuclei, five families of potentials were found for both the scattering of α-particles and for ^3He ions. The obtained optimal parameters of the interaction potential, and the corresponding values of the volume integral of the real part J_V/aA, and the values of χ^2/N are given in Tables 1, 2.

The best agreement with experiment for the nucleus under study for the scattering of α particles is provided by the potentials from the set *A1* (the minimum value of χ^2/N), and at ^3He, by the set *H3* using the combined type of absorption in the imaginary part.

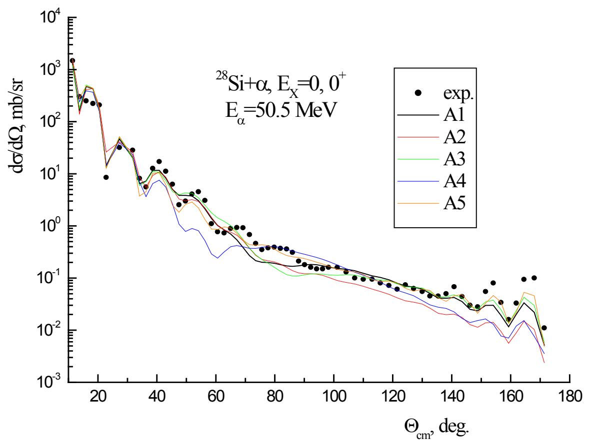

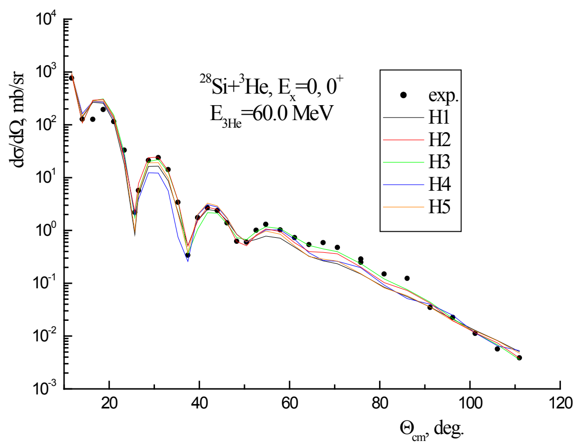

Points – experiment, curves – calculation according to the optical model with potentials from Table 1.

Figure 1 – Elastic scattering of α-particles and ^3He ions by ^{28}Si nuclei

Table 1 – Optical potentials used in calculating elastic and inelastic scattering cross sections for systems $^{28}Si+\alpha$ (E_α=50.5 MeV)

A+a	Set	*V*, MeV	r_V, fm	a_V, fm	*W*, MeV	r_W, fm	a_W, fm	J_V/aA, MeV·fm^3	χ^2/N
$^{28}Si+\alpha$	A1	117.3	1.247	0.808	18.95	1.570	0.718	345	15
	A2	116.5	1.247	0.791	21.94	1.570	0.631	338	27
	A3	123.3	1.247	0.809	19.52	1.570	0.714	363	16
	A4	100.0	1.247	0.809	16.21	1.570	0.838	288	25
	A5	80.0	1.483	0.647	41.94	1.225	0.862	329	11

Table 2 – Optical potentials used in calculating elastic and inelastic scattering cross sections for systems $^{28}Si+^3He$ (E_α=60 MeV)

A+a	Set	*V*, MeV	r_V, fm	a_V, fm	*W*, MeV	r_W, fm	a_W, fm	W_D, MeV	r_D, fm	a_D, fm	J_V/aA, MeV·fm^3	χ^2/N
$^{28}Si+^3He$	H1	102.1	1.15	0.818	25.48	1.44	0.981	-	-	-	337	14
	H2	120.0	1.11	0.860	16.14	1.61	0.648	3.73	1.47	0.866	373	10
	H3	111.2	1.15	0.827	4.80	1.40	0.90	15.59	1.22	0.81	367	8
	H4	106.3	1.09	0.828	8.92	1.32	0.27	9.41	1.48	0.86	310	14
	H5	93.96	1.22	0.781	21.90	1.57	0.865	-	-	-	341	13

A characteristic feature of the measured angular distributions is the well-pronounced nuclear rainbow effects, which are manifested in the presence of a diffraction structure at angles less than 60^0 with a structureless decay of the cross sections with increasing scattering angle. The interpretation of the observed picture becomes more transparent in a semiclassical language. In this case, the differential cross sections at a certain angle are determined by the contribution of the trajectories corresponding to scattering at the "near" and "far" edges of the nucleus. Figure 2 shows an example of the expansion of the theoretical cross section into the near and far components for elastic scattering of α particles at potential *A1* from Table 1 it can be seen that in the range of angles $90 – 140^0$ the experimental cross sections are almost completely reproduced by the far component, and at small and largest angles, where the amplitudes of both components are comparable, pronounced oscillations are observed due to the interference of the amplitudes. Calculation of the far component without absorption shows that the maximum itself and the subsequent decrease are due only to the refractive property of the nuclear field.

The radial dependences of the real and imaginary parts of the nuclear potentials given in Tables 1, 2 and are shown in Figure. 3.

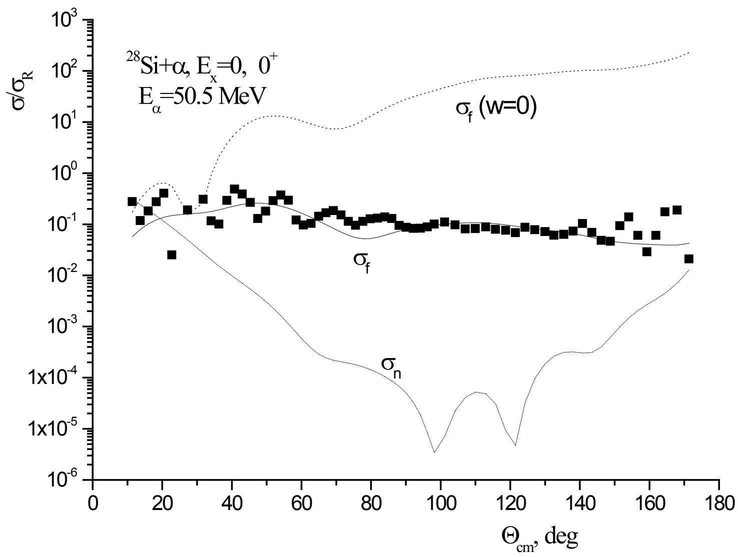

Points are an experimental data. Solid curve is a calculation by the optical model for scattering at the far-edge of the nucleus. The dashed line is the near-edge scattering calculation. The dotted line is the far-edge scattering calculation at zero absorption.

Figure 2 – Disintegration of the theoretical cross section into near and far components for elastic scattering of α-particles by ^{28}Si at an energy of 50.5 MeV

It can be seen that the values of the real and imaginary parts of the potentials differ greatly from each other both at small ($r < 4$ *fm*) and large ($r > 7$ *fm*) distances. But for $r = 6$ *fm*, they intersect. It should be noted that the region near $r = 6$ *fm* corresponds to the strong absorption radius $R_{SA} = 6.05$ *fm*, determined according to [27] by the expression:

$$R_{SA} = \frac{\eta}{k}\left\{1+\left[1+\left(\frac{L_{SA}+1/2}{\eta}\right)^2\right]^{1/2}\right\}, \quad (5)$$

where $k = \sqrt{2mE/\hbar}$ an d$\eta = Z_p Z_t e^2/\hbar v$ is Sommerfeld parameter.

L_{SA} is partial wave for which the absorption coefficient when moving along the Rutherford trajectory $T=1-|S_L|^2=0.5$, where $|S_L|$ is modulus of the S-matrix element for the partial wave L. This condition is fulfilled for $L = 16$ (see Figure 4).

Using the optical potentials of Tables 1 and 2, the experimental data were analyzed by the channel coupling method, where the calculation was carried out taking into account both elastic and inelastic scattering channels with the excitation of the 2^+ and 4^+ states of the nucleus under study in the rotational approximation (calculation code ECIS-88 [28]). The optimal agreement of the calculated values with the experimental data was achieved by varying the parameters V, W and β_2. The analysis results are presented in Figures 5 and 6, where points are an experimental data, solid curves are theoretical calculations. The parameters of the deformation of the nuclei are determined $^{28}Si + \alpha$: $\beta_2 = 0.37$ and for $^{28}Si + {}^3He$: $\beta_2 = 0.49$, close in value to the corresponding values from the work [8].Taking into account only the quadrupole deformation extracted from the $0^+ - 2^+$ bond, a good description of all three experimental data on elastic and inelastic scattering of the cross sections was achieved.

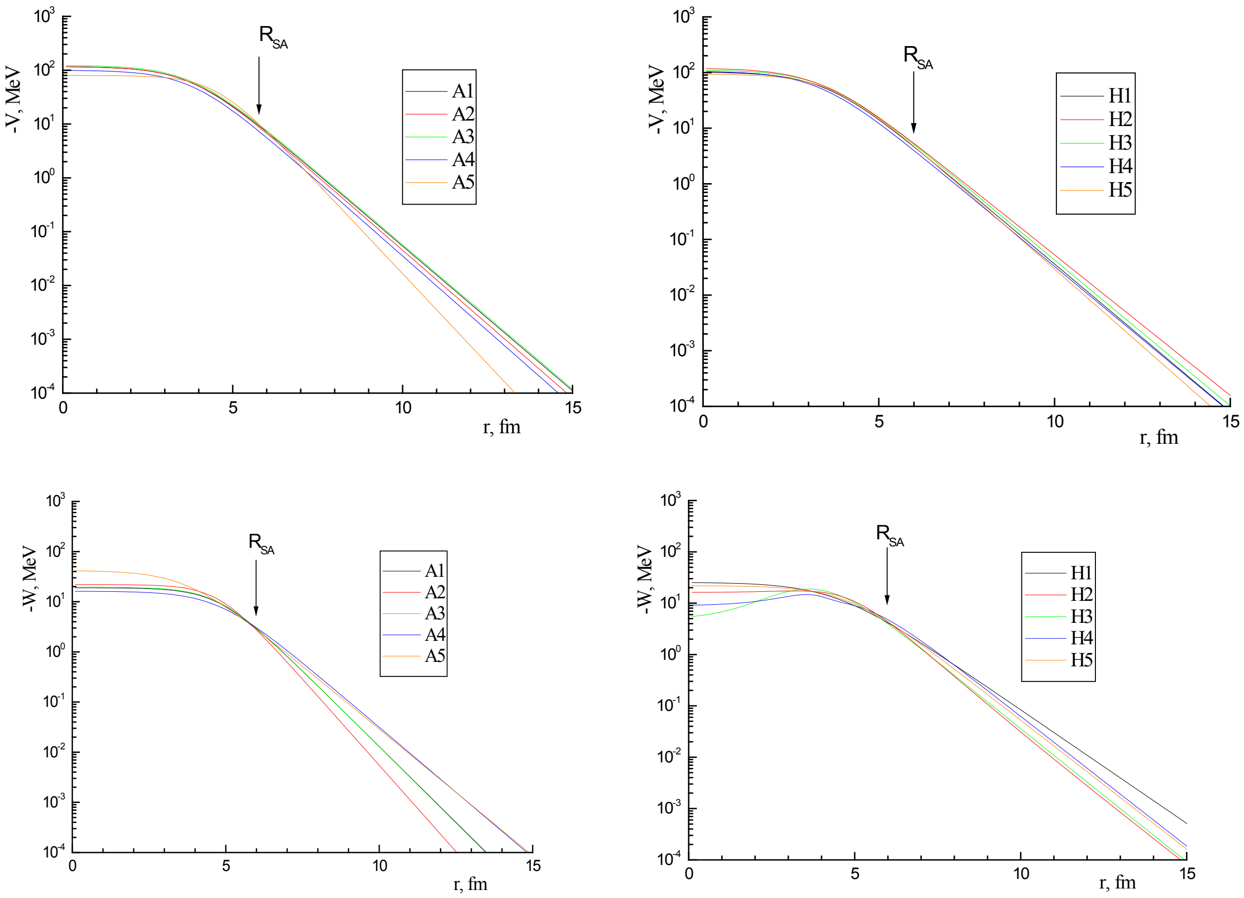

Figure 3 – Radial dependences of real (V) and imaginary (W) nuclear potentials from Tables 1 and 2

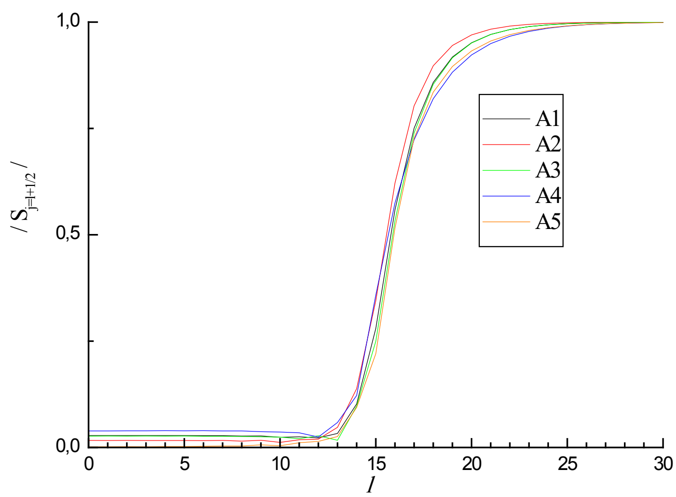

Figure 4 – Scattering matrix elements $|S_{l+1/2}|$ from Table 1

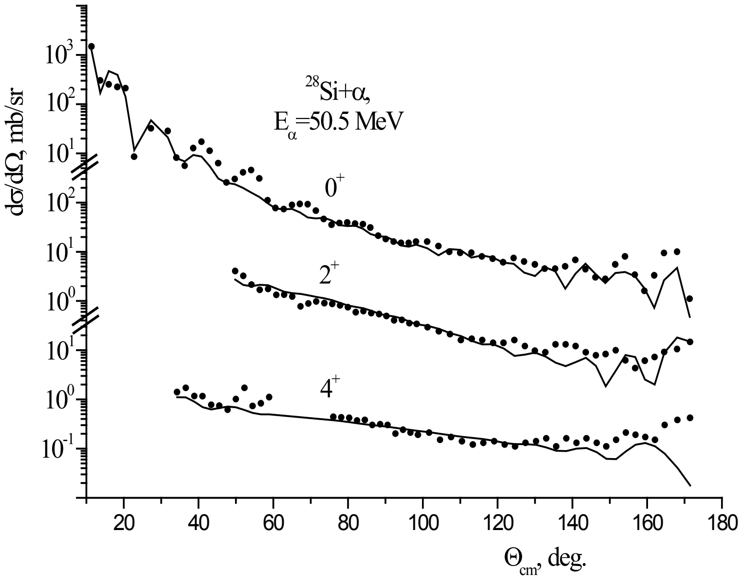

Figure 5 – Angular distributions of elastic and inelastic scattering of α-particles with an energy of 50.5 MeV by ^{28}Si nuclei with level excitation 1.78 MeV (2^+) and 4.61 MeV (4^+)

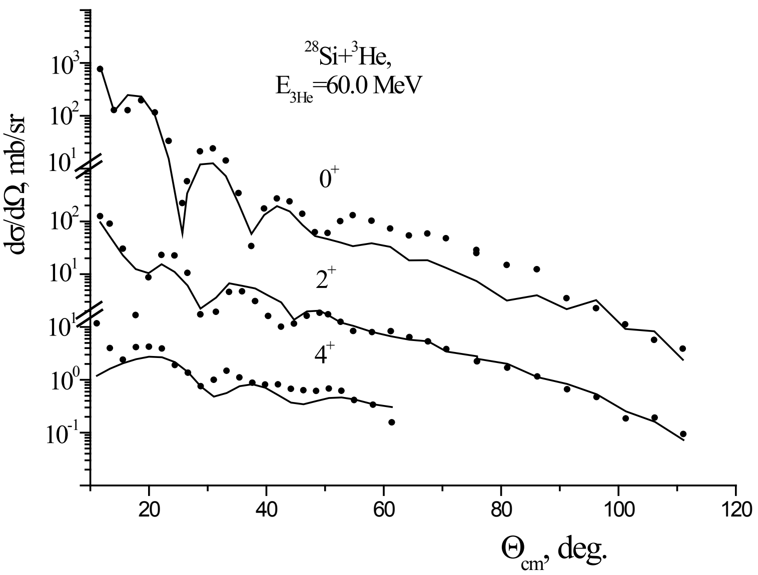

Figure 6 – Angular distributions of elastic and inelastic scattering of 60 MeV ^{3}He ions by ^{28}Si nuclei with excitation of the level 1.78 MeV (2^+) and 4.61 MeV (4^+)

Conclusion

Differential cross sections for elastic and inelastic scattering with excitation of the states of the rotational band of the ground state of ^{28}Si were measured at an α-particle energy of 50.5 MeV and ^{3}He energy of 60 MeV. The angular distributions were analyzed using the optical model and the coupled channel method. In the calculations, the phenomenological Woods-Saxon potentials were used, the parameters of which were sought within the framework of the optical model from the condition of the best description of the experimental data on elastic scattering. In the calculations carried out within the framework of the coupled channel method, a collective model was used.

Optimal values of the parameters of internuclear interaction of colliding particles were found from calculations of experimental data on elastic and inelastic scattering of helium ions by ^{28}Si nuclei within the framework of the optical model and the method of coupled channels. Taking into account the influence of the channel coupling in the calculations made it possible to determine the reliable values of the parameters of the quadrupole deformation, which are in good agreement with the literature data.

Acknowledgements

This research has been funded by the Science Committee of the Ministry of Education and Science of the Republic of Kazakhstan (Grant No. AP08955611).

References

1 Hodgson P.E. The nuclear optical model // Rep. Progress Physics. – 1971. – Vol. 34. – P. 765–819.

2 Sadykov B.M., Zholdybayev T.K., Burtebayev N., et.al. Scattering of α -particles and ^{3}He by ^{24}Mg nuclei at energies about 50–60 MeV. Eur. Phys. J. – 2021. – Vol. A57. – P. 130.

3 Artemov K.R., Brenner M., Golovkov M.S., et.al. Excitation function for the elastic scattering of alpha particles by ^{28}Si and the alpha-cluster structure of the ^{32}S nucleus // Yad. Fiz. – 1992. – Vol. 55. – P. 884.

4 Manngard P., Brenner M., Alam M.M., et.al. Molecular potential and elastic scattering of alpha particles by ^{28}Si from 14 to 28 MeV // Nucl. Phys. – 1989. – Vol. A504. – P. 130.

5 Galanina L.I., Zelenskaya N.S., Konyukhova I.A., et.al. Investigation of the mechanism of inelastic alpha-particle scattering on 28Si nuclei by the method of angular αγ correlations at E=30.3 MeV // Physics of Atomic Nuclei. – 2010. – Vol. 73. – P. 1339–1350.

6 Kwon Y.K., Lee C.S., Kubono S. Elastic scattering of 120-MeV alpha particles by 28Si // Jour. of the Korean Phys. Soc. – 2007. – Vol. 51. – P. 1635.

7 Youngblood D.H., Clark H.L., Lui Y.W. Giant monopole resonance strength in 28Si // Nucl. Phys. – 1998. – Vol. 57. – P. 1134–1144.

8 Berezhnoy Yu.A. and Molev A.S. Airy minima in 4He+28Si elastic and inelastic scattering // Modern Phys. Lett. – 2020. – Vol. A35. – P. 2050159.

9 Kanada-En'yo Y., and Ogata K. Transition properties of low-lying states in Si28 probed via inelastic proton and α scattering // Phys. Rev. – 2020. – Vol. C101. – P. 064607.

10 Adsley P., Nesterenko V.O., Kimura M., et.al. Isoscalar monopole and dipole transitions in ^{24}Mg, ^{26}Mg, and ^{28}Si // Phys. Rev. – 2021. – Vol. C103. – P. 044315.

11 Burtebayev N., Nassurlla M., et.al. Scattering of α-particles by ^{11}B nuclei at an energy of 40 MeV and role of the exchange mechanism with transfer of ^{7}Li // International Journal of Modern Physics. – 2018. – Vol. E27. – P. 1850094.

12 12 Burtebayev N., Duysebayev A., Duysebayev B.A., et.al. Scattering of α-particles and ^{3}He on ^{16}O nuclei and its excitation mechanism at energies near 50 MeV // International Journal of Modern Physics. – 2017. – Vol. E26. – P. 1750018.

13 Leleux P., Macq P.C., Meulders J.P., Pirart C. The (He3,d), (d,p) and (d,n) reactions on 28Si // Zeits. fuer Phys. – 1974. – Vol.271. – P.139.

14 Артемов К.П., Голдберг В.З., Рудаков В.П., Сериков И.Н. Упругое рассеяние ^{3}Не на большие углы // Ядерная Физика. – 1971. – Vol. 13. – P. 268-276.

15 Fulmer C.B., Mariolopoulos G., Bagieu G., et.al. Scattering of 41 MeV alpha particles and 46 MeV He-3 from Al-27, Si-28, Si-29 and Si-30 // Phys. Rev. – 1978. – Vol. C18. – P. 621–631.

16 Willis N., Brissaud I., Le Bornec Y., et.al. Elastic scattering of 217 MeV ^{3}He particles // Nucl. Phys. – 1973. – Vol. 204. – P. 454–464.

17 Yamagata T., Utsunomiya H., Tanaka M., et.al. Elastic scattering of ^{3}He particles at 450 MeV // Nucl. Phys. – 1995. – Vol. 589. – P. 425–434.

18 Burtebayev N., Duisebayev A., Duisebayev B. A., et.al. Elastic and inelastic scattering of α-particles by ^{20}Ne nuclei at energy of 48.8MeV // International Journal of Modern Physics. – 2018. – Vol. E27. – P. 1850042.

19 Буртебаев Н.Т., Дуйсебаев А.Д., Иванов Г.Н. Упругое рассеяние 50 МэВ α-частиц на ядрах ^{14}N, ^{16}O, ^{20}Ne, ^{24}Mg и ^{28}Si // Изв. АН КазССР. Сер. физ.-мат. – 1984. – №6. – С. 49-53.

20 Буртебаев Н.Т., Виноградов А.А., Вонгай А.Д. и др. Система многомерного анализа для исследования ядерных реакций на циклотроне ИЯФ АН КазССР // Изв. АН КазССР. Сер. физ.-мат. – 1975. – № 2. – С. 65-68.

21 Perey F.G. SPI-GENOA an optical model search code // NBI version. – 1976.

22 Avrigeanu M., von Oertzen W., Plompen A. J. M., and Avrigeanu V. Optical model potentials for α-particles scattering around the Coulomb barrier on A∼100 nuclei // Nucl. Phys. – 2003. – Vol. A723. – P. 104–126.

23 Guo H., Xu Y., Liang H., Han Y., and Shen Q. He4 microscopic optical model potential // Phys. Rev. – 2011. – Vol.C83. – P.064618.

24 Pang D.Y., Roussel-Chomaz P., Savajols H., et.al. Erratum: Global optical model potential for A=3 projectiles // Phys. Rev. – 2010. – Vol. C81. – P. 019902.

25 Xu Y., Guo H., Han Y., and Shen Q. Helium-3 global optical model potential with energies below 250 MeV // Physics, Mechanics and Astronomy. – 2011. – Vol. 54. – P. 2005-2014.

26 Devries R.M., Goldberg D.A., Watson J.W., et.al. Transition between light- and heavy- ion elastic scattering // Phys. Rev. Lett. – 1977. – Vol. 39. – P. 450-461.

27 Madurga G., Lozano M., and Jadraque A. (1980) The role of rainbow refraction in heavy ion elastic scattering // Phys. Lett. – 1980. – Vol. B95. – P. 358–360.
28 Raynal J. Computer code ECIS-88 (unpublished).

References

1 P.E. Hodgson, Rep. Prog. Phys. 34, 765-819 (1971).
2 B.M. Sadykov, T.K. Zholdybayev, N. Burtebayev, et.al. Eur. Phys. J. A57, 130 (2021).
3 K.R. Artemov, M. Brenner, M.S.Golovkov, et.al. Yadernaya Fizika, 55(4), 884-889 (1992) (in Russ.).
4 P. Manngard, M. Brenner, M.M. Alam, et.al. Nucl. Phys. A504, 130-142 (1989).
5 L.I. Galanina, N.S. Zelenskaya, I.A. Konyukhova, et.al. Phys. At. Nucl. 73, 1339–1350 (2010).
6 Y.K. Kwon, C.S. Lee, S. Kubono, J Korean Phys. Soc. 51, 1635–1639 (2007).
7 D.H. Youngblood, H.L. Clark, and Y.W. Lui, Phys. Rev. C57, 1134–1144 (1998).
8 Yu.A. Berezhnoy and A.S. Molev, Modern Phys. Lett. A35, 2050159 (2020).
9 Y. Kanada-En'yo, and K. Ogata, Phys. Rev. C101, 064607 (2020).
10 P. Adsley, V.O. Nesterenko, M. Kimura, et.al. Phys. Rev. C 103, 044315 (2021).
11 N. Burtebayev, M. Nassurlla, et.al. Int. J. Mod. Phys. E1850094 (2018).
12 N. Burtebayev, A. Duysebayev, B.A. Duysebayev, et.al. Int. J. Mod. Phys. E26, 1750018 (2017).
13 P. Leleux, P.C. Macq, J.P. Meulders, C. Pirart, Z. Phys. 271, 139-148 (1974).
14 K.P. Artemov, V.Z. Goldberg, V.P. Rudakov, I.N. Serikov, Yadernaya Fizika, 13, 268-276 (1971) (in Russ.).
15 C.B. Fulmer, G. Mariolopoulos, G. Bagieu, et.al. Phys. Rev. C18, 621–631 (1978).
16 N. Willis, I. Brissaud, Y. Le Bornec, B. Tatischeff, and G. Duhame, Nucl. Phys. A204, 454–464 (1973).
17 T. Yamagata, H. Utsunomiya, M. Tanaka, et.al. Nucl. Phys. A589, 425–434 (1995).
18 N. Burtebayev, A. Duisebayev, B.A. Duisebayev, et.al. Int. J. Mod. Phys. E27, 1850042 (2018).
19 N.T. Burtebaev, A. Duysebaev, G.N. Ivanov, Izvestiya Akademii Nauk Kazakh SSR, 6, 49-53 (1984) (in Russ.).
20 N.T. Burtebaev, A.A. Vinogradov, A.D. Vongai, et.al. Izvestiya Akademii Nauk Kazakh SSR, 2, 65-68 (1975) (in Russ.).
21 F.G. Perey, NBI version (1976).
22 M. Avrigeanu, W. von Oertzen, A.J.M. Plompen, and V. Avrigeanu, Nucl. Phys. A723, 104–126 (2003).
23 H. Guo, Y. Xu, H. Liang, Y. Han, and Q. Shen, Phys. Rev. C83, 064618 (2011).
24 D. Y. Pang, P. Roussel-Chomaz, H. Savajols, R.L. Varner, and R. Wolski, Phys. Rev. C81, 019902 (2010).
25 Y. Xu, H. Guo, Y. Han, and Q. Shen, Sci China Phys. Mech. 54, 2005-2014 (2011).
26 R.M. DeVries, D.A. Goldberg, J.W. Watson, M.S. Zisman, and J.G. Cramer, Phys. Rev. Lett. 39, 450–453 (1977).
27 G. Madurga, M. Lozano, and A. Jadraque, Phys. Lett. B95, 358–360 (1980).
28 J. Raynal, Computer code ECIS-88 (unpublished).